Innovations in low UCS core acquisition and quality assessment using digital rock physics

Dmitry Lakshtanov[1], Jennie Cook[1]*, Yuliana Zapata[1], Dave Saucier[1], Robin Eve[1], Mark Lancaster[1], Nathan Lane[1], Glen Gettemy[1], Kevan Sincock[2], Elizabeth Liu[2], Rosemarie Geetan[3], Ian Draper[4], and Tim Gill[4]

[1]BP, Sunbury, UK & Houston, Texas, USA
[2]BP, now independent consultant
[3]BP, now Bifrost Energy
[4]Baker Hughes

Abstract. Digital rock physics was used to support development and deployment of a novel percussion sidewall coring technology that can enable a cost-effective reservoir characterization strategy. Subsurface samples acquired with percussion sidewall core often exhibit penetrative damage making them of limited use for subsurface characterization. We have evaluated a novel method of percussion sidewall core (PSWC) acquisition that minimizes acquisition damage and will provide intact samples of reservoir material for use in subsurface workflows. This paper details the benchmarking and validation workflow developed using laboratory experiments and digital rock physics on outcrop samples. A planned field trial of this technology is planned for 2022.

Six sandstones of known properties were used in the validation program, and these sandstones exhibit a range of low to medium unconfined compressive strengths (UCS). Reference plugs were cut from all materials. The sandstone samples were then used as the source material in laboratory testing of various novel designs of PSWC bullets. The PSWC bullets were shot in simulated downhole environments. Both reference plugs and test plugs were imaged with high-resolution X-ray microCT (Zeiss Versa), and digital rock analysis was conducted on all samples. Using images of reference and post-test material, damage could be identified and simulated petrophysical properties including porosity and permeability could be determined and directly compared.

Digital rock physics provide unique insight to evaluate and quantify changes (or lack of changes) to the sample material subjected to the PSWC acquisition. Damage encountered in the test samples includes grain crushing and compaction that degrades storage and transport properties, and dilatant zones that locally enhance transport properties. The presence, frequency and distribution of these zones are dependent on experimental parameters. In all cases, undisturbed rock fabric could be identified in each sample and intact texture was verified by comparison with reference material.

A novel and efficient method for acquiring and evaluating subsurface samples was developed and benchmarked. By optimizing PSWC bullet design and coupling this with a mature, image-based digital rock technology, this work demonstrates that the samples and results obtained by this method are representative. Based on encouraging results from the validation workflow, the novel percussion sidewall technology will be run in an upcoming carbon capture appraisal well. We will discuss preliminary observations from this field trial with the opportunity to compare the results against full bore and rotary coring.

1 Introduction

Rock samples are a key part of any subsurface workflow, whether traditional oil & gas or carbon capture & sequestration. Rock samples are used as 'ground-truth' in wireline analysis and inform the complete subsurface description. Full bore core offers the most comprehensive sampling strategy, but cost may make acquiring core difficult to justify.

Rotary sidewall core (RSWC) acquired on wireline offers a less costly mechanism to acquire core plugs for subsurface characterization. Although, RSWC may not be suitable for all analyses including relative permeability, recovered cores are generally of good quality and suitable for most routine and special core analysis. However, in weak or highly overbalanced formations, RSWC acquisition can have poor recovery (Jackson, 2021). In such cases, the only alternative is to acquire rock samples via percussion sidewall coring (PSWC). PSWC often has good recovery, but the acquisition process and eventual sample extraction can result in sample damage affecting traditional laboratory analysis (Webster and Dawsongrove, 1959). In routine core analysis, typically the entire width of the PSWC or RSWC sample is used, but it may be trimmed for length. This is especially an issue for soft PSWC samples, where some of the extracted material is likely to be damaged further. Thus, any analysis of the whole extracted plug will likely include both damaged and undamaged regions which may impact analytical measurements.

To reduce the issues associated with PSWC damage, a novel bullet was designed. The main innovations consist in an optimized bullet profile and an X-ray transparent internal sleeve. The bullet profile was modified to reduce stress concentration and minimize damage ahead of the barrel during sample acquisition. The internal sleeve encapsulates the sample reducing the risk of damage during extraction from the barrel assembly. In addition, X-ray transparency allows direct high-resolution imaging of the acquired sample,

enabling the use of Digital Rock Physics (DRP) (Draper et al., 2022; Lakshtanov et al., 2022).

DRP is a technique that uses high-resolution three-dimensional imaging and numerical simulation to determine the static and dynamic properties of an imaged sample. Static properties from DRP can be used in the same way as traditional laboratory core analysis. Unlike laboratory core analysis, however, image-based simulations can be performed on a variety of subsurface samples, from whole and RSWC, but also end trims, offcuts, PSWC, and cuttings, where no other traditional analysis can be used. DRP analysis offers reduced cycle time over most laboratory special core analysis, often providing results within weeks once material is received.

In addition to DRP simulation results, the three-dimensional images can provide critical information, particularly where heterogeneity or sample quality may be an issue. Using DRP, the plug can be imaged, and undamaged regions can be selected, which is why DRP/PSWC for softer reservoirs has been a significant value driver over the last few years.

2 Sample Selection

Six sandstones of known properties were used in the novel PSWC testing program. These sandstones were chosen to cover a wide range of low and medium unconfined compressive strengths (UCS). Reference plugs were cut from all sandstones. The sandstone samples were then used as the parent material in laboratory testing of various designs of PSWC barrels. The novel PSWC barrels were shot in ambient and simulated downhole environments discussed further in section 3.2 (Lakshtanov et al., 2022).

Sandstones included in this study include Silver Sands (SS), Salt Wash South (SO), Salt Wash Red (SW), Castlegate (CG), Berea Buff (BB), and Berea Spider (BS). General rock properties for these formations were provided by the material supplier and are outlined in ***Table 1***.

All formations are generally homogeneous clean quartz sandstones with variable amounts of cement and intergranular clay. Bedding is visible in some samples, particularly the SW formation. Where possible sample blocks were oriented to allow the plugs to be acquired parallel to bedding, as they would be in a typical downhole application (vertical well in horizontal bedding), but in some cases this was not possible, and some plugs were acquired across dipping beds.

Grain density for all samples is between 2.61 and 2.66 g/cm^3 (***Table 1***), indicative of a quartzose grain framework. Cement, where present, typically consists of quartz overgrowths with minor carbonate. Sample porosity and permeability vary between 20% to 35%, and between 100mD to ~10 D, respectively. UCS ranges from weak (<100 psi) to hard (> 5000 psi). A common rule of thumb in the industry to select between RSWC and PSWC methods is to use the target formation expected UCS values. In target formations with UCS lower than 100psi, PSWC is often preferred because of greater sample recovery, whereas where UCS is greater than 1000psi RSWC is usually preferred. There are other considerations in selecting the best acquisition method, including downhole hydrostatic overbalance and intended use of the sample, but UCS is often the primary determining factor. In this study, rock types with UCS values above and below 1000psi were selected to explore the impact of rock properties on sample recovery and quality.

Table 1 : Rock properties for outcrop sandstones included in the novel PSWC evaluation program (Lakshtanov et al., 2022).

Formation	Sample Code	Grain Density (g/cm^3)	Porosity (%)	Permeability (mD)
Berea Buff	BB	2.64	21.4	273
Berea Buff		2.63	21.4	407
Berea Buff		2.63	21.4	402
Berea Buff		2.63	21.7	283
Berea Spider	BS	2.64	21.3	346
Berea Spider		2.63	21.7	428
Castlegate	CG	2.63	26.9	920
Castlegate		2.63	26.9	1100
Castlegate		2.63	27.2	876
Castlegate		2.63	25.6	764
Salt Wash Red	SW	2.63	24.3	1720
Salt Wash Red		2.62	25.4	2370
Salt Wash Red		2.62	24.1	1890
Salt Wash South	SO	2.63	30.2	6590
Salt Wash South		2.61	30.7	6320
Salt Wash South		2.60	31.9	7260
Salt Wash South		2.61	30.9	5550
Silver Sands	SS	2.64	32.1	9185
Silver Sands		2.66	33.8	9158
Silver Sands		2.65	33.1	8291

Porosity versus UCS for the six sandstones included in the testing program are shown in ***Figure 1***. In these clean sandstones, porosity variation is primarily a function of grain packing and cementation, thus high porosity sandstones selected have a looser packing arrangement and less cement and are typically weaker than lower porosity sandstones. UCS was measured on samples from these formations, but we do not have UCS information for each sample evaluated. Because we see good correlation between porosity and UCS for these test plugs (***Figure 1***), for further analyses we use porosity as a proxy for rock strength in this sample suite.

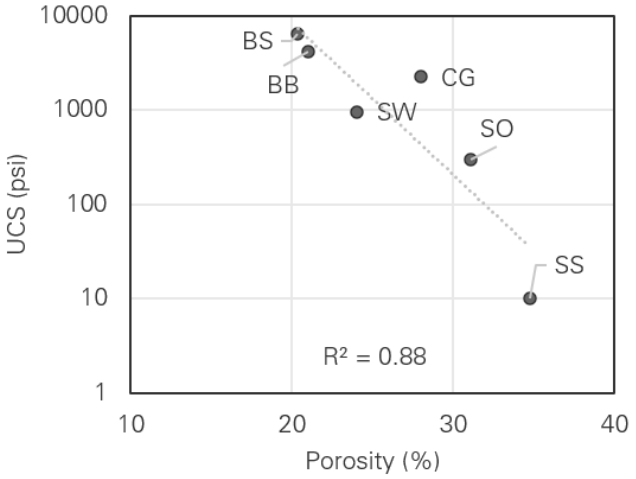

Figure 1 : Porosity and unconfined compressive strength (UCS) for outcrop sandstones included in the PSWC evaluation

3 Novel PSWC Design & Testing

3.1. Barrel & Sleeve Design

The objective of design and testing of the novel PSWC tool was to modify the traditional tool in such a way as to minimize damage to the extracted sample and to facilitate analysis of the recovered material. The design of the novel PSWC barrel was refined over multiple iterations, however all versions differed from conventional PSWC barrels in one key aspect: the addition of an X-ray transparent aluminum sleeve (Draper et al., 2022).

A conventional barrel typically consists of two parts, the driver, and the cutter (***Figure 2***). A key innovation was the addition of an aluminum sleeve (***Figure 2)***. The aluminum material of the sleeve was deliberately chosen to be X-ray transparent to allow microCT scanning of the formation.

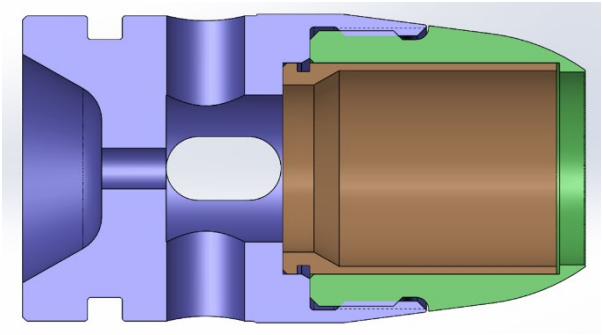

Figure 2 : Novel PSWC barrel assembly including driver (blue), cutter (green), and aluminum sleeve (brown)

When used downhole the three components are assembled as shown in ***Figure 2***. After the core is recovered, the tool is disassembled to allow the sleeve to be removed without disturbing the sample material inside. The sleeve would then be returned to the lab for CT-scanning (Draper et al., 2022).

For this project, the quality of the resultant core was optimized, and a series of tests was conducted to refine the design of the cutter of the barrel to minimize observed damage. The design changes were guided by computer modelling of the formation behavior during the coring process, and several designs were developed and tested. The barrel design ultimately selected for testing and analysis has significantly less metal at the cutter edge than a traditional barrel (***Figure 2***), resulting in a narrower and sharper profile. Through testing, it was determined that this sharper profile significantly reduced damage to the cores.

3.2. Testing Program

Three phases of experimental tests were designed to evaluate the novel percussion sidewall coring tool and its performance and effectiveness under a variety of conditions:

Phase 1: Ambient quasi-static tests
Phase 2: Ambient dynamic tests
Phase 3: Reservoir-condition dynamic tests

3.2.1 Phase 1: Ambient Quasi-static

The objective of Phase 1 was to test the initial barrel assembly concept and design and calibrate penetration versus load data for subsequent dynamic tests. In Phase 1, PSWC barrels were pushed into blocks of outcrop sandstones (CG, SW, and BB) with a 100kN frame at velocities between 20 and 90 m/s. Sleeves and samples were then extracted from the test bullet and photographed and microCT-scanned (Lakshtanov et al., 2022).

3.2.2 Phase 2: Ambient Dynamic

Phase 2 tests were designed to test dynamic penetration of the barrel and improve the design to maximize recovery and minimize sample damage. These tests were conducted at ambient conditions with a transient overbalance applied to the sample face. The team wanted to evaluate the survivability of the barrel assembly, the effectiveness of the internal sleeve, ease of sample removal, and sample damage for different formations acquired at higher velocities (Lakshtanov et al., 2022).

3.2.3 Phase 3: Reservoir-Condition Dynamic

Phase 3 tests were designed to test the acquisition and recovery of sample material with dynamic penetration at reservoir conditions. An Overbalance Test Cell (OBTC) was designed where barrels were fired through pressurized water to evaluate the impact of charge, rock type, pressure, filter cake, and barrel design. Using this design, and adjustable overbalance between 0 – 1000 psi could be applied. All samples were saturated with either base oil or water (SS). Mudcake was simulated variously by layers of primer, paint, and silicone adhesive. Velocity of the bullet was directly measured for both phase 2 and phase 3 tests.

Several key variables were evaluated in Phase 3 test runs (3a, 3c, 3d, 3e), including cell pressure, cell velocity, gun pressure, muzzle velocity, barrel penetration, and length of recovered cores. These runs varied in the types of samples tested, the conditions tested, and test design including sleeve diameter and OBTC feed through. Most tests were conducted at 1000 psi cell pressure, with several tested at lower pressures (200 psi) to evaluate the impact of overbalance. Cell velocity is the velocity of the bullet prior to impact as measured in the OBTC by frangible pins recording the progress of the projectile over time. The gun pressure is the pressure at which the external airgun was fired, whereas the muzzle velocity is the velocity the projectile exiting the gun. Cell velocity is the speed of the barrel just before impact inside the OBTC. Penetration refers to the depth of penetration of the barrel into the sample material, which often correlates to the length of the recovered sample material (Lakshtanov et al., 2022).

4 Digital Rock Physics Imaging & Analysis

4.1. Imaging

High-resolution 3D micro-CT digital rock images of test and reference plugs were acquired using a Zeiss Versa microCT system located in BP's laboratories in Sunbury-on-Thames, United Kingdom. Micro-CT is ideally suited for

DRP imaging because it uses non-destructive X-ray scanning to generate 3D images. The Zeiss Versa micro-CT system enables imaging at multiple resolutions, facilitating sample characterization at multiple scales. Images were acquired at resolutions between 2 and 11 microns and image size was frequently greater than one billion voxels. Each voxel consists of a 16-bit grayscale attenuation value. These X-ray attenuation values are approximately proportional to the material density and chemistry and thus can be interpreted easily (Ketcham and Carlson, 2001; Cnudde and Boone, 2013).

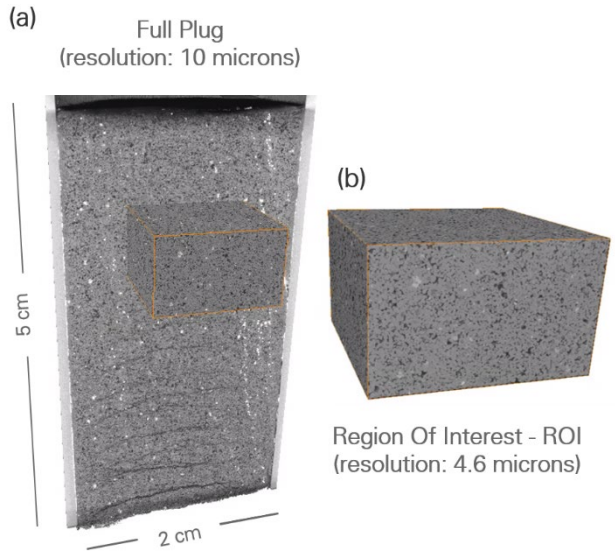

Figure 3: Micro-CT images of acquired sample material (CG). (a) Full plug image at 10 microns including sleeve, and region-of-interest (ROI) image location imaged at 4.6 microns (orange) acquired in an intact portion of the sample. The top of the image is the face of the sample. (b) Region-of-interest (ROI) image (Lakshtanov et al., 2022).

Material that had been tested and extracted as part of the novel PSWC testing program and control material were imaged from each sandstone formation. Where possible, both control and test samples were equally sized, and images were acquired at similar resolutions.

Two types of images were acquired as part of the validation program. Full plug images, where the entire width of the plug was imaged, were acquired typically at resolutions between 7 and 11 microns (***Figure 3***). This type of image is used to assess plug-scale damage, but resolution is not adequate for numerical simulation of rock properties such as porosity & permeability (Lakshtanov et al., 2022).

For numerical simulation of rock properties, region-of-interest (ROI) images were acquired at resolutions between 4 – 5 microns, with some higher resolution images also acquired (***Figure 3***). In conventional microCT imaging, image resolution is a function of sample size. ROI images are acquired using magnification objectives enabling higher resolution images to be acquired without subsampling the recovered cores. Where possible, these ROI images were acquired from zones identified within full plug images where visible damage was minimal or absent.

4.2. Damage Characterization

Full plug images were used to characterize visible damage to the plug and to locate intact, undamaged areas for ROI imaging and simulation. The damage typically encountered in the test plugs includes open fractures and zones of disaggregation, or grain crushing and zones of compaction. Often this damage occurs perpendicular to the plug axis and orthogonal to the direction of acquisition, but damage also occurs along the edge of the sample at the boundary of the PSWC bullet. This damage along the boundary between bullet and sleeve is often compactive and/or cataclastic and is referred to as a damage 'rind' (Lakshtanov et al., 2022).

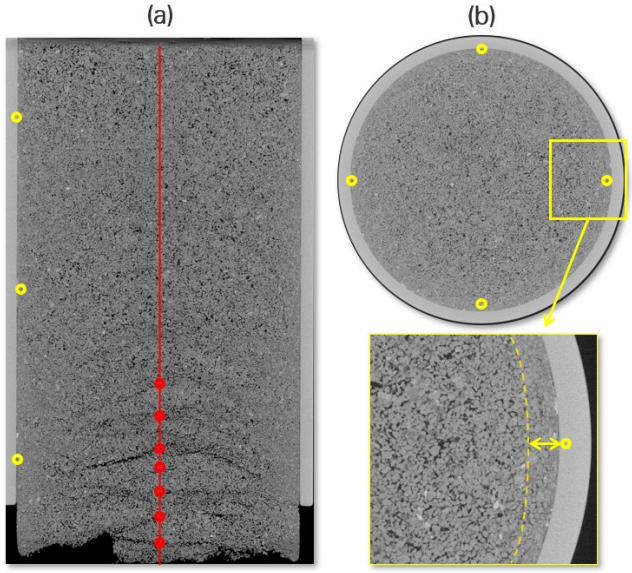

Figure 4 : Damage characterization key metrics: (a) open fractures and cataclastic zones are identified along a transect (red line) along the plug's (CG) length; (b) the rind thickness (compacted/crushed zone) is measured in several locations along the xy plane and the sample's length (yellow circles) (Lakshtanov et al., 2022).

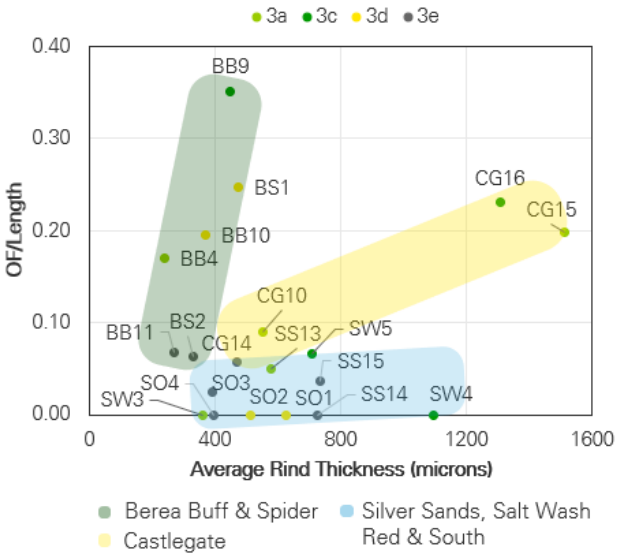

Figure 5: OF/length vs average rind thickness for Phase 3 (Reservoir-condition dynamic) test runs (Lakshtanov et al., 2022).

To characterize the observed damage, three indexes were compared across the various experiments. These indexes are: (1) average rind thickness, (2) open fracture ratio, and (3) cataclastic zone ratio. The average rind thickness is calculated as the average thickness of the visible damage at the sleeve boundary measured at three locations along the

plug's length (bottom, center, top) and the xy plane (north, south, east, and west). The open fracture and cataclastic zone ratios are computed as the number of fractures/ cataclastic zones encountered divided by the plug's length. The main damage metrics and occurrence in a test plug is shown in ***Figure 4*** and the two ratios are shown graphically in ***Figure 5***. Clustering among formation samples is observed and highlighted by the colored clouds in the plot. The clustering trends are associated with similar rock properties among the formation samples such as porosity and UCS.

The effects of sample length on the observed damage at the boundary of the sample (average rind thickness) for various formations are explored in ***Figure 6***, also shown clustered by formation. Longer samples within the same formation appear to exhibit a thicker damage rind around the edge. Some variation is evident where samples were tested with modified sleeve designs (i.e., CG14).

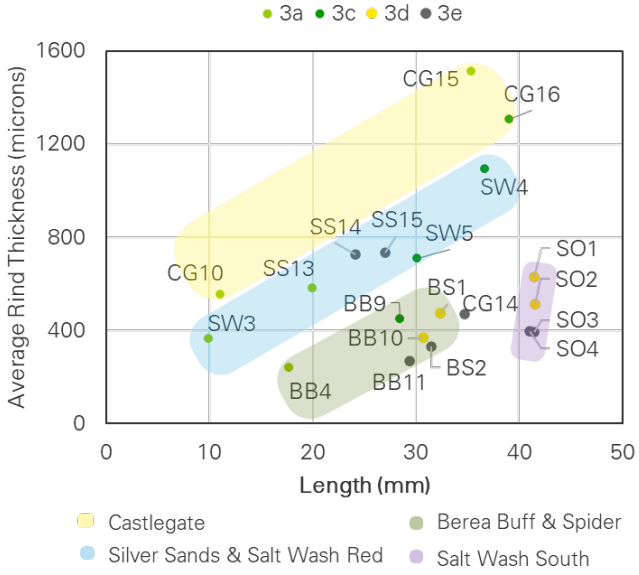

Figure 6: Average rind thickness vs. plug length for different series 3a, 3c, 3d, and 3e. The sample length and the observed damage exhibit a positive correlation associated with each formation (Lakshtanov et al., 2022).

Relationships between damage indices and select experimental parameters are explored in ***Figure 7***. These plots show that plug velocity and penetration impact the amount of damage encountered in these plugs, but the type, amount, and distribution of damage is highly dependent on formation and rock properties.

Intact zones were chosen for high-resolution ROI imaging and DRP simulation. Intact zones were identified visually and characterized by the absence of cataclasis or open fractures and were often located near the center of the acquired sample.

4.3. Static Property Simulation

Prior to DRP numerical simulation, ROI images were processed to reduce noise, enhance coherence, and preserve grain edges. Post-filtering, the images were segmented based on the X-ray attenuation into pore and grain phases. To segment the image, we employed a region-growing thresholding algorithm (Caselles et al., 1997, Sheppard et al., 2004; Jones et al., 2007).

The segmented image is then used as a numerical grid for parallelized image-based Direct Numerical simulations (Fredrich et al., 2014), part of BP's DRP workflow. Methods and results from our image-based petrophysical property simulations have gone through a rigorous verification and validation process as discussed in detail in Fredrich et al. (2014).

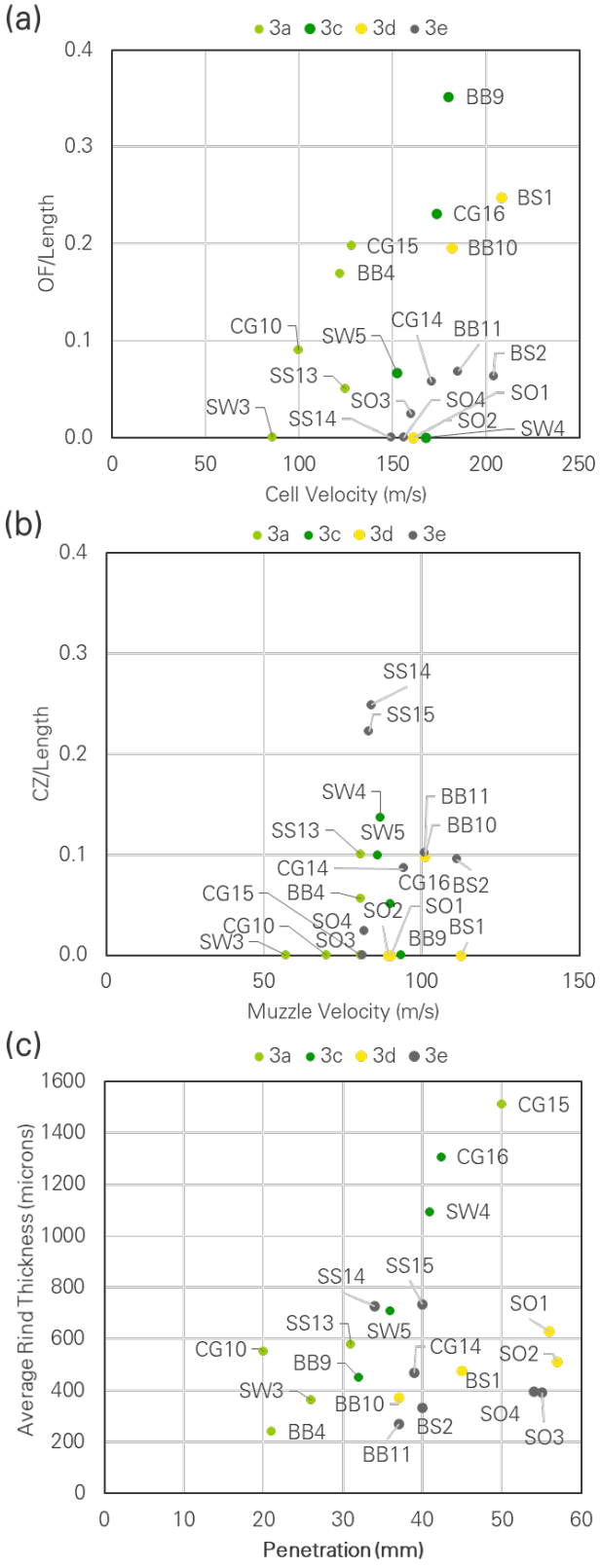

Figure 7: Damage metrics & experiment variable controls for various series of experiments. (a) open fracture ratio and cell velocity, (b) cataclastic zone ratio and muzzle velocity, (c) average rind thickness and penetration (Lakshtanov et al., 2022).

Both reference and test samples were imaged at high-resolution and processed through BP's internal DRP

workflow. Image-based porosity & permeability results were directly compared between reference and test samples, and routine core analysis results, where available.

DRP porosity versus permeability for both reference (control) and test samples are shown in ***Figure 8***. Properties vary with formation and span a porosity range of over 15 porosity units and over two of orders of magnitude permeability. SS and SO samples have the highest porosity & permeability whereas BS and BB have the lowest porosity & permeability. To compare results more directly from reference (control) and test plugs, we averaged porosity and permeability for each test series and formation and plotted it against averaged porosity and permeability for the reference sample results for the same formation. These averaged results are presented in ***Figure 9*** for Phase 3 tests.

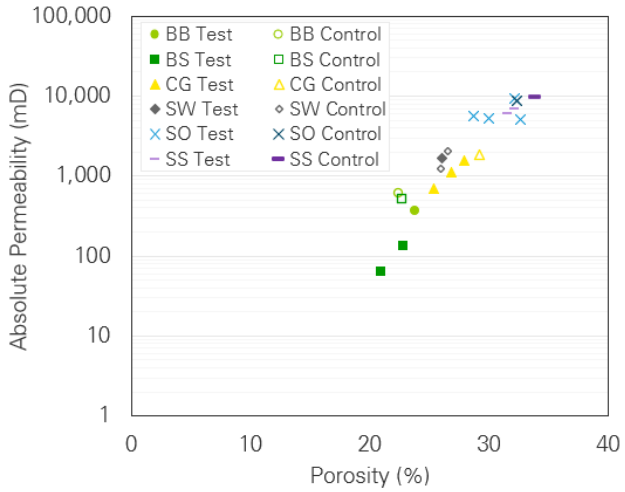

Figure 8: Permeability and porosity for various test and control plugs (Lakshtanov et al., 2022).

Digital rocks physics results for control samples and those acquired via test acquisition offer the best opportunity to compare changes to the sample fabric and texture. Although there is natural variability present in these samples that cannot be excluded, averaged results are within 5 porosity units and within one order of magnitude permeability between plugs extracted through the PSWC process and control plugs.

Routine core analysis was performed on reference material of all formations and provided in T***able 1***. Samples were dried at 105°C. Porosity was measured using a porosimeter at 1.3 MPa confining pressure. Permeability was measured with a porosimeter at 2.7 MPa confining pressure, whereas DRP properties were acquired at ambient conditions. Averaged RCA porosity and permeability versus DRP control and test sample porosity and permeability are shown in ***Figure 10***.

5 Field Trialing the Novel PSWC Technology

Based on encouraging results from the laboratory testing and DRP evaluation, the next step in the novel PSWC development will be testing the tool in a downhole environment in a real formation. Wells targeting softer formations where this tool is likely to be used in the future have been prioritized.

Field trials of the novel percussion tool are scheduled to occur in 2022 and 2023. Where possible, multiple types of subsurface samples will be acquired including full bore core and/or rotary sidewall core (RSWC) to provide a robust comparison. Traditional RSWC or full-bore core samples will be sent for both traditional routine laboratory core analysis (RCA) and digital rocks analysis. Novel PSWC will be analyzed with the Digital Rocks workflow and RCA where possible, and results compared to traditional core acquisition methods.

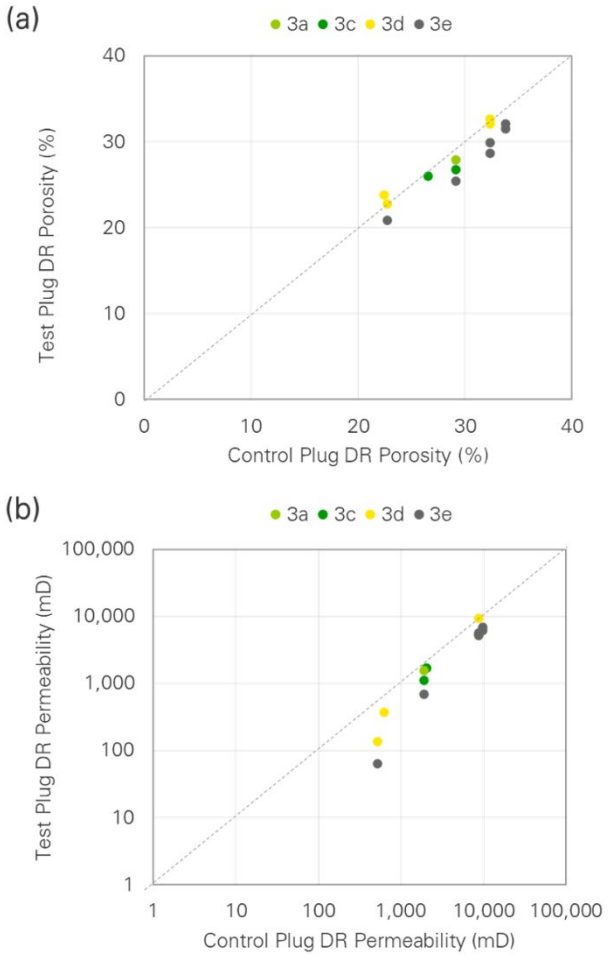

Figure 9: Control and test plug property comparison by experiment series: (a) porosity, (b) permeability (Lakshtanov et al., 2022).

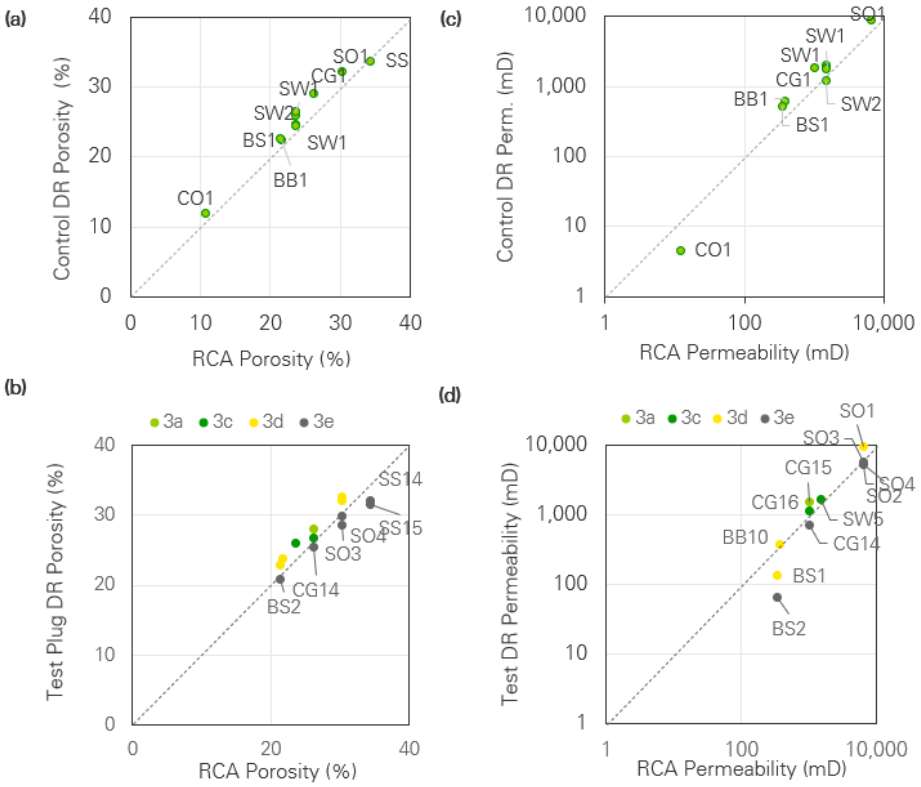

Figure 10: Control and test plugs comparison between laboratory (RCA) and DRP static properties. (a) Control DRP and RCA porosity, (b) Test DRP and RCA porosity, (c) Control DRP and RCA permeability, (d) Test DRP and RCA permeability.

6 Summary & Conclusions

Traditional PSWC have long been considered of limited value. However, with modification to the PSWC tool and barrel it is possible to acquire high quality cores that can be used as inputs into digital rock analysis. This solution is best suited for lower and moderate UCS formations.

In this paper we demonstrate ongoing validation and benchmarking of a novel percussion sidewall coring technique using DRP, a high-resolution three-dimensional image-based workflow. We characterize plug-scale damage with full plug imaging and introduce a semi-quantitative damage characterization scheme. We use these full plug images to identify areas with minimal visible damage for high-resolution ROI imaging to compute static rock properties for both test and control plugs.

The results show that although all samples tested with the novel percussion sidewall coring technique exhibit damage at the plug scale, internally, these plugs contain intact be analyzed in subsurface workflows with DRP.

The ability to couple percussion sidewall coring with DRP analysis in soft sands will enable a low-cost sampling strategy for traditional oil & gas and carbon capture & sequestration applications. BP has developed and maintained a mature DRP technology capability with in-house imaging and analysis capabilities for subsurface characterization workflows. This technology capability ensures that both the acquisition and analysis of PSWC is cost effective.

Next steps for this project include a field trial of the tool coupled with DRP analysis on plugs extracted from whole core and those extracted with the novel percussion sidewall coring technique. We anticipate these field trials occurring in 2022 & 2023.

References

1. Caselles, V., R. Kimmel, and G. Sapiro, 1997, Geodesic active contours, International Journal of Computer Vision, vol. 22, no. 1, p. 61-79.

2. Cnudde, V. and M. Boone, 2013, High-resolution X-ray computed tomography in geosciences: A review of the current technology and applications, Earth-Science Reviews, vol. 123, p. 1-17.

3. Draper, I., T. Gill, D. Lakshtanov, J. Cook, Y. Zapata, R. Eve, M. Lancaster, N. Lane, D. Saucier, G. Gettemy, and K. Sincock, Solving the challenge of acquiring low UCS cores for quantitative digital rock physics, SPWLA 63rd Annual Logging Symposium, https://doi.org/10.30632/SPWLA-2022-0128

4. Lakshtanov, D., Y. Zapata, D. Saucier, J. Cook, R. Eve, M. Lancaster, N. Lane, G. Gettemy, K. Sincock, E. Liu, R. Geetan, I. Draper, and T. Gill, 2022, Using digital rock physics to evaluate novel percussion core quality, SPWLA 63rd Annual Logging Symposium, https://doi.org/10.30632/SPWLA-2022-0128

5. Fredrich, J. T., D. Lakshtanov, N. Lane, E. B. Liu, C. Natarajan, D. M. Ni, and J. Toms, 2014, Digital

Rocks: Developing An Emerging Technology Through To A Proven Capability Deployed In The Business, SPE 170752.

6. Jackson, C. 2021. Tutorial: A Century of Sidewall Coring Evolution and Challenges, From Shallow Land to Deep Water. Petrophysics 62 (03), 230-243, https://doi.org/10.30632/PJV62N3-2021t1

7. Jones, A. C., C. H. Arns, A. P. Sheppard, D. W. Hutmacher, B. K. Milthorpe, and M. A. Knackstedt, 2007, Assessment of bone ingrowth into porous biomaterials using MICRO-CT, Biomaterials, vol. 28, no. 15, p. 2491-2504.

8. Ketcham, R. A. and W. D. Carlson, 2001, Acquisition, optimization and interpretation of X-ray computed tomographic imagery: applications to the geosciences, Computers & Geosciences, vol. 27, no. 4, p. 381-400.

9. Sheppard, A. P., R. M. Sok, and H. Averdunk, 2004, Techniques for image enhancement and segmentation of tomographic images of porous materials, Physica A: Statistical mechanics and its applications, vol. 339, no. 1, p. 145-151.

10. Webster, G. M., & Dawsongrove, G. E. 1959. The Alteration of Rock Properties by Percussion Sidewall Coring. Paper SPE 1159-G prepared for presentation at Fall Meeting of Los Angeles Basin Section in Los Angeles, California, October 16-17, https://doi.org/10.2118/1159-G